

NUMERICAL SIMULATION OF SOLITON PROPAGATION WITH VARIABLE DEPTH

Manuel R. Alfonso^a, Walter E. Legnani^{a,b} and Franco M. Pessana^{a,c}

^a*Centro de Procesamiento de Señales e Imágenes, Facultad Regional Buenos Aires, Universidad Tecnológica Nacional, Medrano 951, 1179, CABA, malfonso0@gmail.com*

^b*Instituto de Cálculo, Universidad de Buenos Aires, Av. Intendente Cantilo S/N, 1428, CABA, walter@ic.fcen.uba.ar, www.ic.fcen.uba.ar.*

^c*Facultad de Ciencias Exactas y Naturales, Universidad Favaloro, Belgrano 1723, C.A.B.A., Argentina, <http://www.favaloro.edu.ar>*

Keywords: Soliton, variable depth Korteweg and de Vries equation, Spectral Methods, Exponential Time Differencing method.

Abstract. The numerical simulation of long wave propagation is extendedly studied in the literature. The effects on the shape, speed and amount of energy carried by this type of waves have an important significance in many scientific and technological applications. In particular the propagation of solitons, this turned on the eye of the scientific community due to the events of the past ten years. When a soliton travels in the middle of the sea, the bottom is disregarded in order to understand the propagatory behavior mechanisms.

In this work we show what happens when a soliton reaches the beach, when the depth of the sea becomes lower. Many other configurations of the bottom had been studied to understand how to design efficient coastal defenses to avoid the destructive effects of the Tsunamis.

To carry out with the studies, a high resolution numerical scheme based upon spectral methods has been designed and implemented to solve the Korteweg and de Vries equation with variable depth.

The results constitute a remarkable contribution in the field of the numerical simulation of fluid mechanics, and show a few applications in other fields like bioengineering and communication with optic fibers.

1 INTRODUCTION

The propagation of solitary waves has attracted an increasing amount of people since the beginning of 1970. Their existence in a variety of physical scenarios, and their application in optic fiber transmission are of the most attractive features. But the last decade another phenomenon grew in importance. Tsunamis, like the one that hit in the Indian Ocean in December 2004, attract an increasing number of people in the scientific community.

Solitary particle–waves, also called the ‘light bullets’, are localized space–time excitations $\Psi(x, t)$, propagating through a certain medium Ω with constant velocity \mathbf{v} . They describe a variety of nonlinear wave phenomena in one dimension playing important roles in optical fibers, many branches of physics, chemistry and biology.

This phenomenon was first described by John Scott Russell who observed a solitary wave in the Union Canal in Scotland. He found it to be an independent dynamic entity moving with a constant shape and speed. [Russell \(1844\)](#) reproduced the phenomenon in a wave tank and named it the "Wave of Translation"; Demonstrating four facts:

- Solitary waves have the shape

$$asech^2(k(x - vt))$$

- A sufficiently large initial mass of water produces two or more independent solitary waves;
- Solitary waves cross each other “without change of any kind”;
- A wave of height \mathbf{a} travelling in a channel of depth \mathbf{h} has a velocity given by the expression

$$v = \sqrt{g(h + a)},$$

where \mathbf{k} is a constant of propagation, \mathbf{x} the space, \mathbf{t} the time and \mathbf{g} is the acceleration of gravity, implying that a large amplitude solitary wave travels faster than one of low amplitude. Due to the particle like interaction of this solitary wave, [Zabusky and Kruskal \(1965\)](#) coined the term soliton.

In a computer laboratory equipped with accessible platforms is easy to generate numerical solitons and design their propagation in many scenarios, so is cheaper to acquire solid knowledge in the behavior of the solitons propagation and all linked concepts ([Ivancevic and Ivancevic, 2007](#)).

One way to generate solitons is solving nonlinear wave equations that admit this kind of solitary wave as possible solutions of them. The nonlinear wave equation of Korteweg and de Vries ([Kortweg and de Vries, 1895](#)), named as KdV, is well known and with the appropriate initial conditions admits solitary waves and in particular solitons as their solutions. But in order to simulate the effect of waves driven to a coast one must use a modified version of this equation. In this case the “variable-depth” KdV ([Cascaval, 2003](#); [Demiray, 2010](#)).

The time spent in many computer simulations of solitons propagation and interaction is really high. For that reason, spectral and pseudospectral numerical schemes are recommended in the spatial integration of the KdV ([Whitham, 1974](#); [Drazin and Johnson, 1989](#)).

There are a few different ways to integrate spatially the KdV equation ([Trefethen, 2000](#); [Canuto et al, 2007](#); [Krogstad, 2005](#)), in this work we used a pseudo spectral method for the spatial integration and exponential time differentiation method (ETD) ([Kassam and Trefethen, 2005](#); [Cox and Matthews, 2002](#); [De la Hoz, and Vadillo, 2008](#)) for time integration.

In order to know the effects in the change of shape (amount of mass) and velocity of the wave by the interaction of a soliton with a coastline, we develop and implement a high

precision numerical spectral scheme to study this kind of phenomena.

2 KDV AND VARIABLE DEPTH KDV – MODEL EQUATIONS

Some derivations of the variable-depth KdV equation that allow a bottom profile (such as a coast) can be found in the literature (Demiray, 2010; Cascaval, 2003). In this work we use the one derived by Demiray (2011) for its simplicity.

In his work, Demiray (2011) defines a solitary wave of constant depth h_0 , as a progressive wave of permanent shape consisting of a single elevation above the undisturbed free surface, whose amplitude a and the effective length L_0 , are such that $\epsilon=a/L_0$ and h_0^2/L_0^2 are comparatively small quantities.

He considers a two dimensional incompressible non-viscous fluids in a constant gravitational field \mathbf{g} . The space coordinates are denoted by $(\mathbf{x}^*, \mathbf{z}^*)$ and the corresponding velocity components by $(\mathbf{u}^*, \mathbf{w}^*)$. The gravitational force is assumed to be acting along negative z-axis, Figure 1. The equations describing the motion of such a fluid are:

$$\frac{\partial u^*}{\partial x^*} + \frac{\partial w^*}{\partial z^*} = 0 \tag{1}$$

$$\frac{\partial u^*}{\partial t^*} + u^* \frac{\partial u^*}{\partial x^*} + w^* \frac{\partial u^*}{\partial z^*} + \frac{1}{\rho_f} \frac{\partial P^*}{\partial x^*} = 0 \tag{2}$$

$$\frac{\partial w^*}{\partial t^*} + u^* \frac{\partial w^*}{\partial x^*} + w^* \frac{\partial w^*}{\partial z^*} + \frac{1}{\rho_f} \frac{\partial P^*}{\partial z^*} + \mathbf{g} = 0, \tag{3}$$

where ρ_f is the mass density and $\mathbf{P}^*(\mathbf{x}^*, \mathbf{z}^*)$ is the pressure function of the fluid. Assuming that the flow is irrotational, the velocity vector can be derived from a scalar potential $\phi^*(\mathbf{x}^*, \mathbf{z}^*, t^*)$ as

$$u^* = \frac{\partial \phi^*}{\partial x^*}, \quad w^* = \frac{\partial \phi^*}{\partial z^*}. \tag{4}$$

Then, the incompressibility condition reduces to

$$\frac{\partial^2 \phi^*}{\partial x^{*2}} + \frac{\partial^2 \phi^*}{\partial z^{*2}} = 0, \tag{5}$$

and the Euler equation becomes

$$\frac{P^* - P_0}{\rho_f} = -\frac{\partial \phi^*}{\partial t^*} - \frac{1}{2} \left[\left(\frac{\partial \phi^*}{\partial x^*} \right)^2 + \left(\frac{\partial \phi^*}{\partial z^*} \right)^2 \right] - \mathbf{g}z^*, \tag{6}$$

where \mathbf{P}_0 is an integration constant and can be considered as the atmospheric pressure.

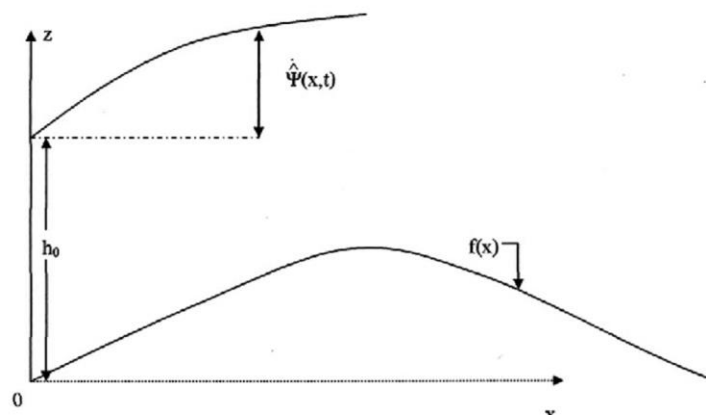


Figure 1. Geometry of the general wave propagation problem in dimensionless coordinates. (Demiray, 2011).

Considering the case of the fluid of height $\mathbf{h}^*(\mathbf{x}^*)$ bounded by a steady atmospheric pressure \mathbf{P}_0 . Let the upper surface of the fluid be described by $\mathbf{z}^* = \psi^*(\mathbf{x}^*, t^*)$ (Figure 1). Then the kinematic boundary condition on this surface reads

$$\frac{\partial \phi^*}{\partial z^*} = \frac{\partial \psi^*}{\partial t^*} + \frac{\partial \phi^*}{\partial x^*} \frac{\partial \psi^*}{\partial x^*} \text{ on } z^* = \psi^*. \quad (7)$$

From the condition (6), the dynamical boundary condition on this surface becomes

$$\frac{\partial \phi^*}{\partial t^*} + \frac{1}{2} \left[\left(\frac{\partial \phi^*}{\partial x^*} \right)^2 + \left(\frac{\partial \phi^*}{\partial z^*} \right)^2 \right] + g\psi^* = 0 \text{ on } z^* = \psi^*. \quad (8)$$

Finally, the lower boundary is supposed to be rigid. Therefore, at $\mathbf{z}^* = \mathbf{h}^*(\mathbf{x}^*) = -\mathbf{h}_0 + \mathbf{f}^*(\mathbf{x}^*)$, the normal velocity component must vanish

$$\frac{\partial \phi^*}{\partial z^*} - \frac{d\mathbf{f}^*}{dx^*} \frac{\partial \phi^*}{\partial x^*} = 0 \text{ on } z^* = -h_0 + f^*(x^*). \quad (9)$$

Here $\mathbf{f}^*(\mathbf{x}^*)$ is the profile function at the bottom of the channel.

At this stage it is convenient to introduce the following non-dimensional quantities

$$\begin{aligned} \phi^* &= c_0 h_0 \hat{\phi}, & \psi^* &= h_0 \hat{\psi}, & x^* &= h_0 x, & z^* &= h_0 z, \\ t^* &= \frac{h_0}{c_0} t, & f^*(x^*) &= h_0 f(x), & c_0 &= \sqrt{h_0 g}, \end{aligned} \quad (10)$$

where c_0 is the phase speed of the linearized wave equation. Introducing (10) into the field Eqs, (5), (7), (8), (9), the following non-dimensional equations are obtained

$$\frac{\partial^2 \hat{\phi}}{\partial x^2} + \frac{\partial^2 \hat{\phi}}{\partial z^2} = 0, \quad (11)$$

$$\frac{\partial \hat{\phi}}{\partial z} = \frac{\partial \hat{\psi}}{\partial t} + \frac{\partial \hat{\phi}}{\partial x} \frac{\partial \hat{\psi}}{\partial x} \text{ on } z = \hat{\psi}. \quad (12)$$

$$\frac{\partial \hat{\phi}}{\partial t} + \frac{1}{2} \left[\left(\frac{\partial \hat{\phi}}{\partial x} \right)^2 + \left(\frac{\partial \hat{\phi}}{\partial z} \right)^2 \right] + g\hat{\psi} = 0 \text{ on } z = \hat{\psi}. \quad (13)$$

$$\frac{\partial \hat{\phi}}{\partial z} - \frac{df}{dx} \frac{\partial \hat{\phi}}{\partial x} = 0 \text{ on } z = -1 + f(x). \quad (14)$$

2.1 Long-wave approximation

Taking the long-wave in shallow water approximation of the above equation by applying the reduction perturbation method, the following stretched coordinates must be introduced

$$\xi = \epsilon^{1/2}(x - t), \quad \tau = \epsilon^{3/2}t, \quad (15)$$

where ϵ is the smallness parameter.

For future purposes we introduce the following new dependent variables:

$$\hat{\phi} = \epsilon^{3/2}\phi, \quad \hat{\psi} = \epsilon\psi. \quad (16)$$

Introducing (16) into the fields Eqs (11) to (14) we obtain

$$\frac{\partial^2 \phi}{\partial z^2} + \epsilon \frac{\partial^2 \phi}{\partial \xi^2} = 0, \quad (17)$$

$$\frac{\partial \phi}{\partial z} = \epsilon \left(-\frac{\partial \psi}{\partial \xi} + \epsilon \frac{\partial \psi}{\partial \tau} \right) + \epsilon^2 \frac{\partial \phi}{\partial \xi} \frac{\partial \psi}{\partial \xi} \text{ on } z = \epsilon\psi, \quad (18)$$

$$-\frac{\partial \phi}{\partial \xi} + \epsilon \frac{\partial \phi}{\partial \tau} + \frac{1}{2} \epsilon \left(\frac{\partial \phi}{\partial \xi} \right)^2 + \frac{1}{2} \left(\frac{\partial \phi}{\partial z} \right)^2 + \psi = 0 \text{ on } z = \epsilon\psi, \quad (19)$$

$$\frac{\partial \phi}{\partial z} - \epsilon \frac{\partial f}{\partial \xi} \frac{\partial \phi}{\partial \xi} = 0 \text{ on } z = -1 + f(x). \quad (20)$$

Now, we expand the functions ϕ and ψ into a suitable power series of ϵ as

$$\begin{aligned} \phi &= \phi_0 + \epsilon \phi_1 + \epsilon^2 \phi_2 + \dots, \\ \psi &= \psi_0 + \epsilon \psi_1 + \epsilon^2 \psi_2 + \dots. \end{aligned} \quad (21)$$

Introducing (21) into the Eqs. (17) to (20), considering that $\mathbf{f}(\mathbf{x})$ is of the form $\mathbf{f}(\mathbf{x}) = \epsilon \mathbf{h}(\xi)$, and setting the coefficients of like power of ϵ equal to zero, we obtain the following sets of differential equations:

O(1) equations:

$$\frac{\partial^2 \phi_0}{\partial z^2} = 0, \quad \frac{\partial \phi_0}{\partial z} \Big|_{z=0} = 0, \quad -\frac{\partial \phi_0}{\partial \xi} + \frac{1}{2} \left(\frac{\partial \phi_0}{\partial z} \right)^2 \Big|_{z=0} + \psi_0 = 0. \quad (22)$$

O(ϵ) equations:

$$\begin{aligned} \frac{\partial^2 \phi_1}{\partial z^2} + \frac{\partial^2 \phi_0}{\partial \xi^2} = 0, \quad \frac{\partial \phi_1}{\partial z} + \psi_0 \frac{\partial^2 \phi_0}{\partial z^2} + \frac{\partial \psi_0}{\partial \xi} = 0, \quad \text{at } z = 0, \\ \left[-\frac{\partial \phi_1}{\partial \xi} - \psi_0 \frac{\partial^2 \phi_0}{\partial z \partial \xi} + \frac{\partial \phi_0}{\partial \tau} + \frac{1}{2} \left(\frac{\partial \phi_0}{\partial \xi} \right)^2 + \frac{\partial \phi_0}{\partial z} \frac{\partial \phi_1}{\partial z} \right] \Big|_{z=0} + \psi_1 = 0, \\ \left[\frac{\partial \phi_1}{\partial z} + h(\xi) \frac{\partial^2 \phi_0}{\partial z^2} \right] \Big|_{z=-1} = 0. \end{aligned} \quad (23)$$

O(ϵ^2) equations:

$$\begin{aligned} \frac{\partial^2 \phi_2}{\partial z^2} + \frac{\partial^2 \phi_1}{\partial \xi^2} = 0, \\ \frac{\partial \phi_2}{\partial z} + \psi_0 \frac{\partial^2 \phi_1}{\partial z^2} + \frac{1}{2} \psi_0^2 \frac{\partial^3 \phi_0}{\partial z^3} + \psi_1 \frac{\partial^2 \phi_0}{\partial z^2} + \frac{\partial \psi_1}{\partial \xi} - \frac{\partial \psi_0}{\partial \tau} - \frac{\partial \phi_0}{\partial \xi} \frac{\partial \psi_0}{\partial \xi} = 0, \text{ at } z = 0, \\ -\frac{\partial \phi_2}{\partial \xi} - \psi_0 \frac{\partial^2 \phi_1}{\partial \xi \partial z} - \frac{1}{2} \psi_0^2 \frac{\partial^3 \phi_0}{\partial z^2 \partial \xi} - \psi_1 \frac{\partial^2 \phi_0}{\partial z \partial \xi} + \frac{\partial \phi_1}{\partial \tau} + \psi_0 \frac{\partial^2 \phi_0}{\partial z \partial \tau} \\ + \frac{\partial \phi_0}{\partial \xi} \left(\frac{\partial \phi_1}{\partial \xi} - \psi_0 \frac{\partial^2 \phi_1}{\partial z \partial \xi} \right) + \frac{1}{2} \left(\frac{\partial \phi_1}{\partial z} + \psi_0 \frac{\partial^2 \phi_0}{\partial z^2} \right)^2 \\ + \frac{\partial \phi_0}{\partial z} \left(\frac{\partial \phi_2}{\partial z} + \psi_0 \frac{\partial^2 \phi_1}{\partial z^2} + \frac{1}{2} \psi_0^2 \frac{\partial^3 \phi_0}{\partial z^3} + \psi_1 \frac{\partial^2 \phi_0}{\partial z^2} \right) + \psi_2 = 0, \text{ at } z = 0, \\ \frac{\partial \phi_2}{\partial z} + h(\xi) \frac{\partial^2 \phi_1}{\partial z^2} - \frac{\partial h}{\partial \xi} \frac{\partial \phi_0}{\partial \xi} = 0, \text{ at } z = 1. \end{aligned} \quad (24)$$

2.2 Solution of the field equations

From the solution of the set of differential Eq. (22) and the associated boundary condition we obtain

$$\phi_0 = \varphi(\xi, \tau), \quad \psi_0 = \frac{\partial \varphi}{\partial \xi}, \quad (25)$$

where $\varphi(\xi, \tau)$ is an unknown function whose governing equation will be obtained later.

To obtain the solution of O(ϵ) equations, given in (23), we introduce the solution (25) into the differential equation (23) to have

$$\begin{aligned} \frac{\partial^2 \phi_1}{\partial z^2} + \frac{\partial^2 \varphi}{\partial \xi^2} = 0, \quad \frac{\partial \phi_1}{\partial z} \Big|_{z=0} + \frac{\partial^2 \varphi}{\partial \xi^2} = 0, \\ \left[-\frac{\partial \phi_1}{\partial \xi} + \frac{\partial \varphi}{\partial \tau} + \frac{1}{2} \left(\frac{\partial \varphi}{\partial \xi} \right)^2 \right] \Big|_{z=0} + \psi_1 = 0, \quad \frac{\partial \phi_1}{\partial z} \Big|_{z=-1} = 0. \end{aligned} \quad (26)$$

The solution of the Eq (26), along with the use of the boundary condition yields

$$\phi_1 = \frac{1}{2} \frac{\partial^2 \varphi}{\partial \xi^2} (z^2 + 2z) + \varphi_1, \quad \psi_1 = \frac{\partial \varphi_1}{\partial \xi} - \frac{1}{2} \left(\frac{\partial \varphi}{\partial \xi} \right)^2 - \frac{\partial \varphi}{\partial \tau}, \quad (27)$$

where $\varphi_1(\xi, \tau)$ is another unknown function whose governing equation will be obtained later.

To obtain the solution for $O(\epsilon^2)$ equation given in (24), we introduce the solutions (25) and (27) into the Eq. (24), to have

$$\begin{aligned} \frac{\partial^2 \phi_2}{\partial z^2} - \frac{1}{2} \frac{\partial^4 \varphi}{\partial \xi^4} (z^2 + 2z) + \frac{\partial^2 \varphi_1}{\partial \xi^2} &= 0, \\ \frac{\partial \phi_2}{\partial z} - 3 \frac{\partial \varphi}{\partial \xi} \frac{\partial^2 \varphi}{\partial \xi^2} + \frac{\partial^2 \varphi_1}{\partial \xi^2} - 2 \frac{\partial^2 \phi_1}{\partial \xi \partial \tau} &= 0, \text{ at } z = 0, \\ -\frac{\partial \phi_2}{\partial \xi} + \frac{\partial \varphi}{\partial \xi} \frac{\partial^3 \varphi}{\partial \xi^3} + \frac{\partial \varphi}{\partial \xi} \frac{\partial \varphi_1}{\partial \xi} + \frac{1}{2} \left(\frac{\partial^2 \varphi}{\partial \xi^2} \right)^2 + \frac{\partial \varphi_1}{\partial \tau} + \psi_2 &= 0, \text{ at } z = 0 \\ \frac{\partial \phi_2}{\partial z} + h(\xi) \frac{\partial^2 \varphi}{\partial \xi^2} - \frac{\partial h}{\partial \xi} \frac{\partial \varphi}{\partial \xi} &= 0, \text{ at } z = -1. \end{aligned} \quad (28)$$

The solution of (28) along with the use of the boundary condition yields

$$\phi_2 = \frac{1}{24} \frac{\partial^4 \varphi}{\partial \xi^4} (z^4 + 4z^3) - \frac{1}{2} \frac{\partial^2 \varphi_1}{\partial \xi^2} z^2 + \left(3 \frac{\partial \varphi}{\partial \xi} \frac{\partial^2 \varphi}{\partial \xi^2} - \frac{\partial^2 \varphi_1}{\partial \xi^2} + 2 \frac{\partial^2 \phi_1}{\partial \xi \partial \tau} \right) z + \varphi_2(\xi, \tau), \quad (29)$$

where $\varphi_2(\xi, \tau)$ is another unknown function whose governing equation will be obtained from the solution of higher order equations.

The use of the last boundary condition of (29) yields the following evolution equation

$$\frac{\partial^2 \varphi}{\partial \xi \partial \tau} + \frac{3}{2} \frac{\partial \varphi}{\partial \xi} \frac{\partial^2 \varphi}{\partial \xi^2} + \frac{1}{6} \frac{\partial^4 \varphi}{\partial \xi^4} - \frac{1}{2} h(\xi) \frac{\partial^2 \varphi}{\partial \xi^2} - \frac{1}{2} \frac{\partial h}{\partial \xi} \frac{\partial \varphi}{\partial \xi} = 0,$$

or, in terms of the function ψ_0 , it reads

$$\frac{\partial \psi_0}{\partial \tau} + \frac{3}{2} \psi_0 \frac{\partial \psi_0}{\partial \xi} + \frac{1}{6} \frac{\partial^3 \psi_0}{\partial \xi^3} - \frac{1}{2} \frac{\partial}{\partial \xi} [h(\xi) \psi_0] = 0. \quad (30)$$

When the function $h(\xi)$ is equal to zero, the evolution equation reduces to the conventional KdV equation

$$\frac{\partial \psi_0}{\partial \tau} + \frac{3}{2} \psi_0 \frac{\partial \psi_0}{\partial \xi} + \frac{1}{6} \frac{\partial^3 \psi_0}{\partial \xi^3} = 0. \quad (31)$$

The equation has the following progressive wave solution

$$\psi_0 = a \operatorname{sech}^2(\zeta), \quad \zeta = \frac{\sqrt{3a}}{2} \left(\xi - \frac{a}{2} \tau \right), \quad (32)$$

where a is the amplitude of the solitary wave.

To our knowledge, there is no analytical solution in the literature of the Eq. (30). Therefore, in what follows we shall present a numerical solution for the variable depth KdV equation.

3 NUMERICAL SCHEMES FOR THE SOLUTION OF THE KDV EQUATION

In (Alfonso and Legnani, 2011; Alfonso et al, 2012) we discussed different appropriate methods for integrating numerically the KdV equation, with the exponential time differencing method with a Runge-Kutta 4 scheme (ETDRK4) arose as the best option.

If the equation is written as

$$u_t + L(u) + N(u) = 0, \quad (33)$$

where \mathbf{L} is a linear operator and \mathbf{N} is a nonlinear operator, with periodic boundary conditions. The ETD method proposed by Kassam and Threfethen (2005) is similar to the Integrating Factor method (IF) (Krogstad, 2005; Tang et al, 2009), if we proceed as in the IF approach and apply the same integrating factor (L =Fourier Linear term derivative) and then integrate over a single time step, we get

$$u_{n+1} = e^{Lh}u_n + \int_0^h e^{-L\tau}N(u(t_n + \tau), t_n + \tau)d\tau, \quad (34)$$

where now h is the time step used. The expression (34) is exact, and the various order ETD schemes come from how one approximate the integral.

The work (Cox and Mathews 2002) presents a sequence of recurrence expressions that provide higher and higher-order approximations of a multistep type. They also derived a set of ETD methods based on Runge-Kutta time-stepping, which they call ETDRK schemes.

The Cox and Mathews ETDRK4 formulation is:

$$\begin{aligned} a_n &= e^{Lh/2}u_n + L^{-1}(e^{Lh/2}u_n - I)N(u_n, t_n) \\ b_n &= e^{Lh/2}u_n + L^{-1}(e^{Lh/2}u_n - I)N(a_n, t_n + h/2) \\ c_n &= e^{Lh/2}u_n + L^{-1}(e^{Lh/2}u_n - I)(2N(b_n, t_n + h/2) - N(u_n, t_n)) \\ u_{n+1} &= e^{Lh}u_n + h^{-2}L^{-3}\{[4 - Lh + e^{Lh}(4 - 3Lh + (Lh)^2)]N(u_n, t_n) \\ &\quad + 2[2 + Lh + e^{Lh}(-2 + Lh)](N(a_n, t_n + h/2) + N(b_n, t_n + h/2)) \\ &\quad + [-4 - 3Lh - (Lh)^2 + e^{Lh}(4 - Lh)]N(c_n, t_n + h)\} \end{aligned} \quad (35)$$

In the expansion (35) is useful to define the following coefficients

$$\begin{aligned} \alpha &= [4 - Lh + e^{Lh}(4 - 3Lh + (Lh)^2)] \\ \beta &= [2 + Lh + e^{Lh}(-2 + Lh)] \\ \gamma &= [-4 - 3Lh - (Lh)^2 + e^{Lh}(4 - Lh)] \end{aligned} \quad (36)$$

Unfortunately, in this form (35), the ETDRK4 proposed by Cox and Mathews (2002) suffer from numerical instability.

All three coefficients in (36) suffer disastrous cancellation errors when L has eigenvalues close to zero. This vulnerability to cancellation errors in the high-order ETD and ETDRK schemes can render them effectively useless for problems which have small eigenvalues in the discretized linear operator (Klein, 2008).

The coefficients in expression (36) have the form of a function of complex variables, $\mathbf{f}(\mathbf{z})$, which are analytic except for a removable singularity at $\mathbf{z} = 0$, this is the main mathematical reason that ruins the stability of the method.

The solution found by Kassam and Trefethen (2005) was to evaluate the function $\mathbf{f}(\mathbf{z})$ via an integral over a contour in the complex plane that encloses z and is well separated from zero. Contour integrals of analytic functions in the complex plane are easy to evaluate by means of the trapezoidal rule.

In the special case of KdV in one dimension (1D) the contour integral reduces to a simple mean of $\mathbf{f}(\mathbf{z})$ over a contour, that was approximated by a mean over equally spaced points along the contour.

4 NUMERICAL EXPERIMENTS

Different coastline profiles were developed to study the approach of the soliton wave. All experiments were designed in a physical framework of a channel of 10 m depth and 150 m long, simulation time was about 50 seconds. In the numerical experiments the model equation was integrated in dimensionless variables.

The numerical implementation was made in MATLAB® 2010b. For all the experiments we solved the KdV equation with initial condition

$$u(x, t) = a \operatorname{sech}^2(\zeta), \quad \zeta = \frac{\sqrt{3a}}{2}(x - x_0), \quad (37)$$

with $a=5$, $x_0=30$, used previously by [Martinez et al \(2010\)](#).

Among the different bottom profiles developed, [Figure 2](#) shows the simplest ones: A simple beach like Slope, which start with a constant depth h_0 and then it change constantly to the size of the soliton wave, this is useful for a first approach solution in which one can see at simple view the variation of speed and profile vs. bottom height. A step like function coast, in which a sudden change of depth is made, this allows us to simulate a break in bottom continuity condition. A Valley like coast, in which a sudden change of h_0 is made and later returns to initial depth. And finally, a comparison with an artery stenosis like bottom profile is used.

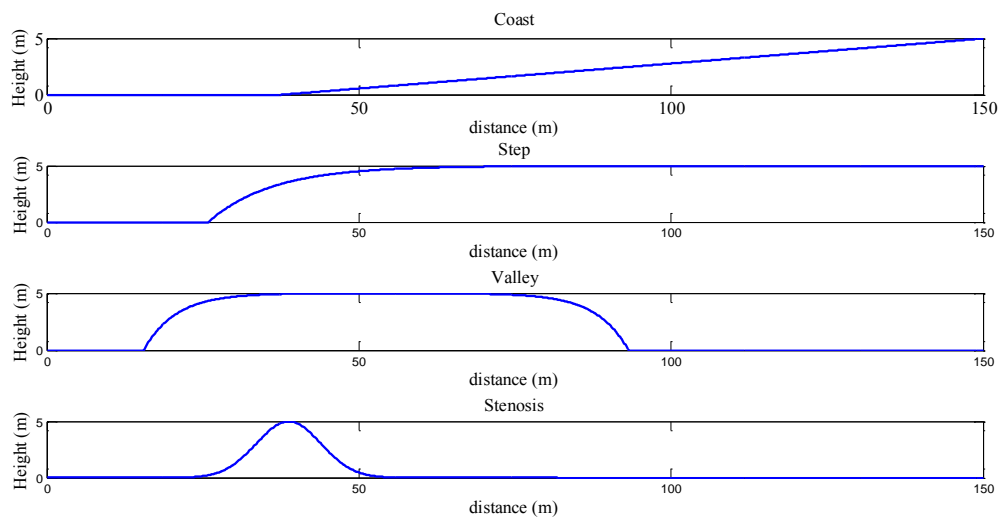


Figure 2. Different coastline profiles studied.

With the aim of reduce and increase the relative height of the free surface depth, the experiments were performed taking a relative positive and negative level coasts described before. Each case was compared with the constant depth solution to analyze the variation of wave speed and shape.

5 RESULTS

With the model presented before and used the numerical scheme ETDRK4 the results obtained are presented below.

5.1 Slope

[Figure 3](#) shows the evolution a soliton with a bottom profile of a positive slope (left) and negative slope (right) vs. the constant depth soliton. It can be seen that when the bottom depth (h_0) decreases, the soliton grows higher and narrows, but its velocity is decreased (remember that the velocity of the soliton is proportional to its height and depth (h_0)). Vice versa in front of an increase of bottom height, the wave speedup but its amplitude is reduced. The comparison between the positive and negative case with the case of constant depth can be seen in [Figure 4](#) for simplicity.

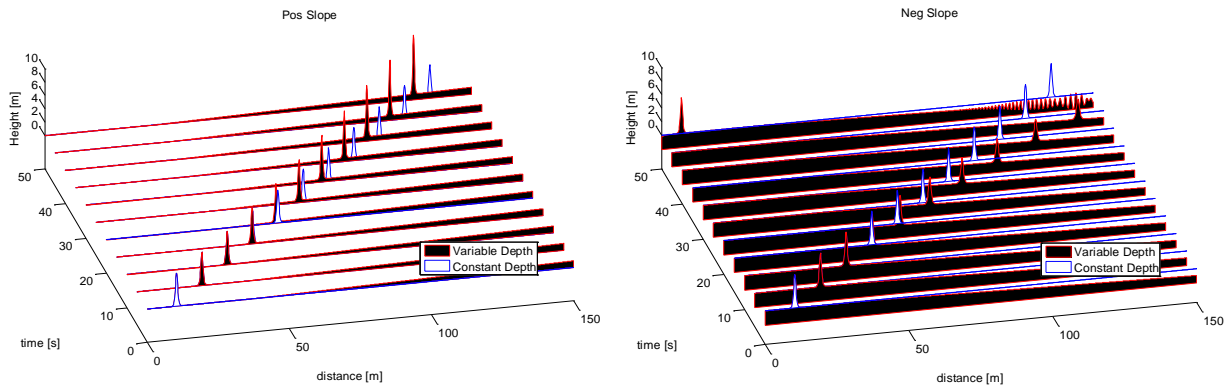


Figure 3. Positive slope (decrease of h_0) left. Negative slope (increase of h_0) right.

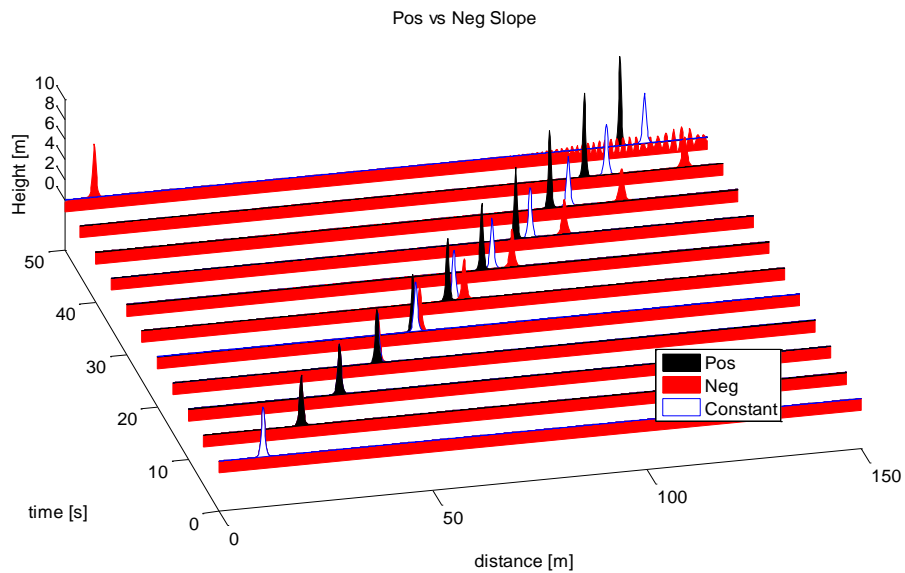


Figure 4. Positive and negative slope vs. constant depth.

5.2 Step

Figure 5 (left) and (right) shows the simulation of a step like function bottom profile. A less pronounced profile is used to avoid generations of reflected waves. Figure 6 shows the comparison for simplicity.

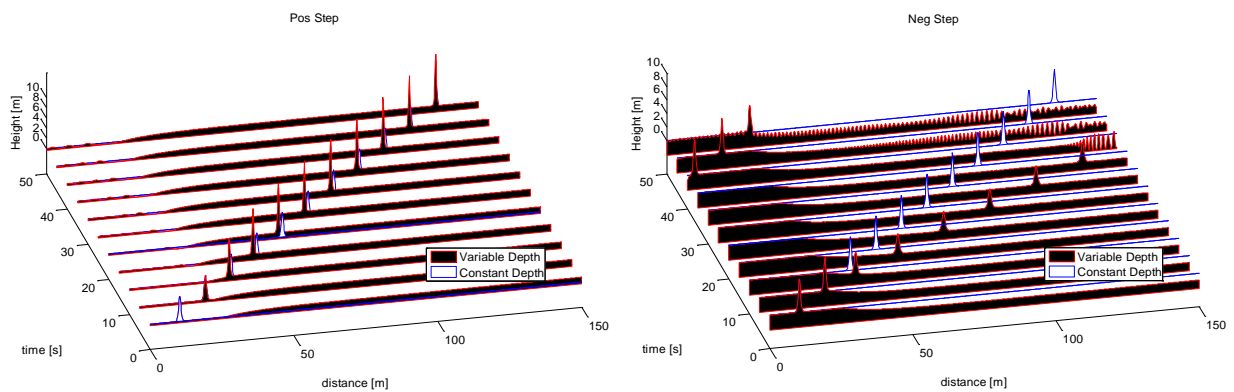


Figure 5. Positive step (decrease of h_0) left. Negative step (increase of h_0) right.

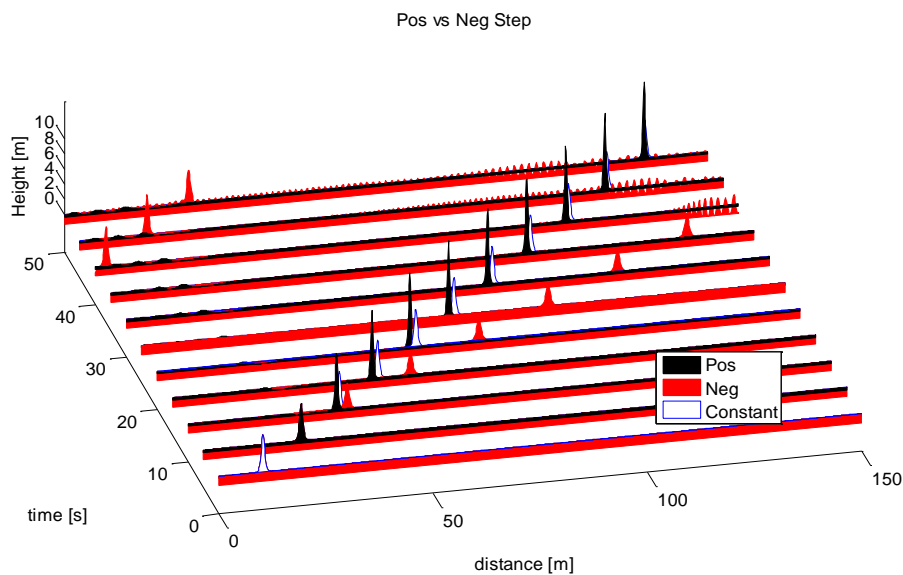


Figure 6. Positive and negative step bottom vs. constant depth

5.3 Valley

Figure 7 left and right show the simulation of a bottom decrease and increase, simulating a valley and a plateau. Again a less pronounced profile is used. A comparison of these profiles is shown in Figure 8.

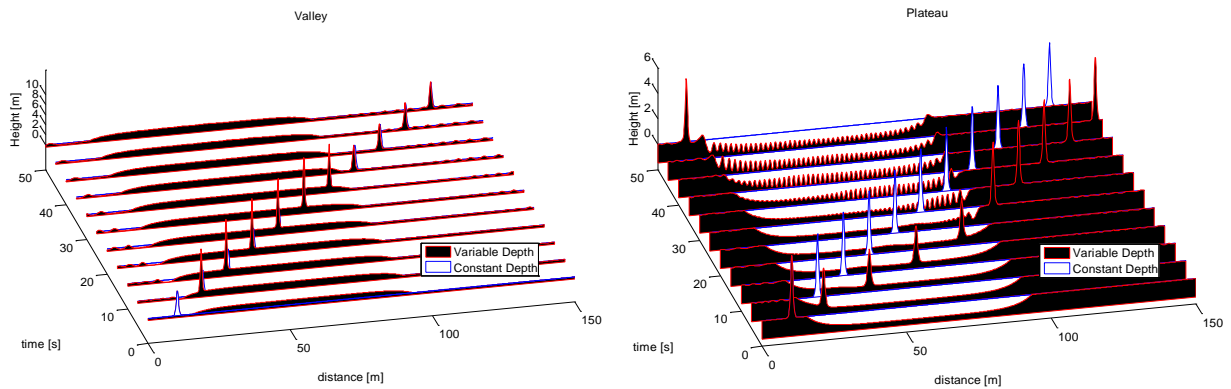


Figure 7. Valley (decrease of h_0) left. Plateau (increase of h_0) right.

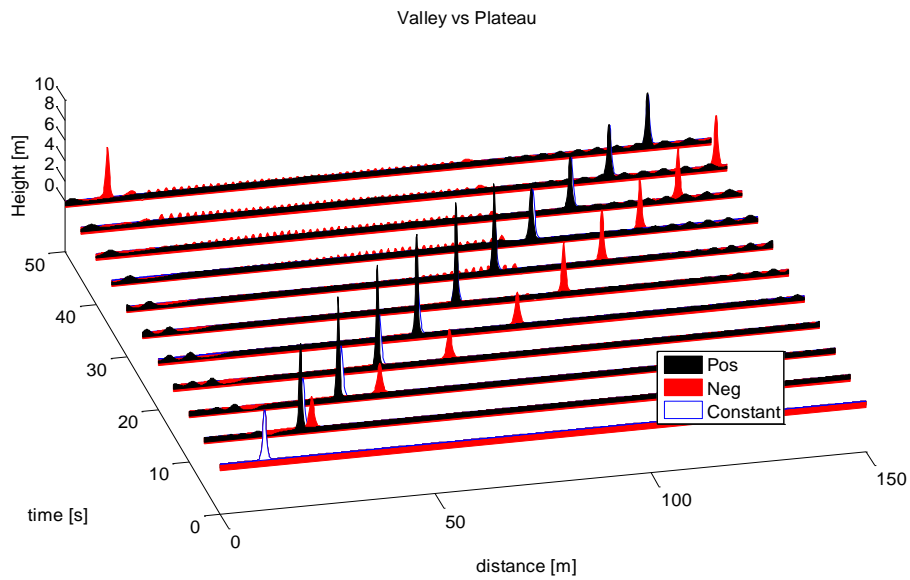


Figure 8. Valley and plateau bottom vs. constant depth

5.4 Stenosis

The final profile is a simulation of an artery stenosis and how this affects the profile and speed. In Figure 9 one can see an increase of the wave amplitude, which will produce more stress in the wall. Only for comparison, a negative stenosis is generated and reproduced in Figure 10.

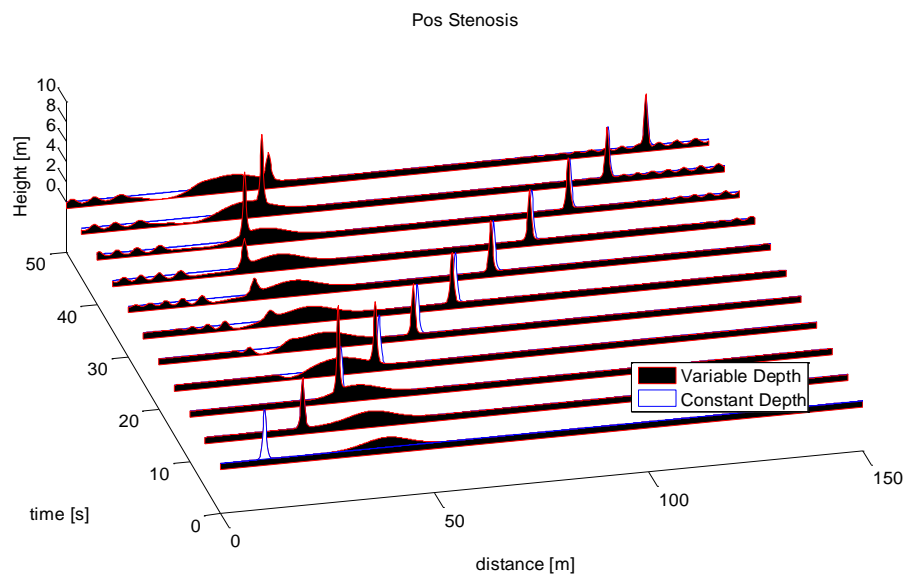


Figure 9. Stenosis like profile. The increase of amplitude can be seen as a higher stress in the wall.

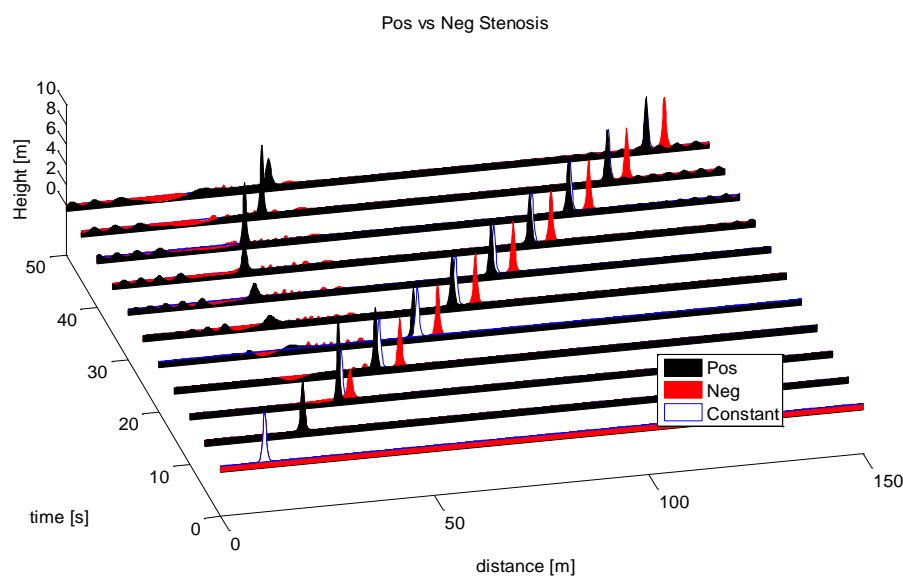


Figure 10. Only for comparison a negative stenosis is performed.

All results show consistently that in the transition of a change in the bottom condition, a change in shape and speed is produced. But when the transitions ends, the wave goes back to its original speed (only for positive change), preserving the end shape.

6 CONCLUSION

We developed a realistic simulation model that can lend us to develop coastline profile that can provide protection against a tsunami wave. All profile models show how difficult is to change the final shape and speed of the wave. In all cases one must decide in a final taller but slower wave or a smaller and faster one.

7 REFERENCES

- Alfonso, M., Legnani, W., A numerical study for improving time step methods in Pseudospectral schemes applied to the Korteweg and De Vries equation. *Mecánica Computacional Vol XXX*, págs. 2763-2775, 2011.
- Alfonso, M., Legnani, W., Pessana, F., Performance indicators of spectral schemes using wavelets applied to numerical integrate the KdV equation. X World Congress in Computational Mechanics, Sao Pablo, Brasil, 8-13 July, 2012.
- Canuto, C.G., Hussaini, M.Y., Quarteroni, A., Zang, T.A., *Spectral Methods: Evolution to Complex Geometries and Applications to Fluid Dynamics*, 1st ed. Springer, 2007.
- Cascaval, R., *Variable Coefficient KdV Equations and Waves in Elastic Tubes. Evolution Equations Lecture Notes in Pure and Applied Mathematics*, vol. 234, pp. 57–69, Dekker, New York, NY, USA, 2003.
- Cox, S.M., Matthews, P.C., Exponential time differencing for stiff systems. *J. Comput. Phys.* 176, 430–455, 2002.
- De la Hoz, F., Vadillo, F., An exponential time differencing method for the nonlinear Schrödinger equation. *Computer Physics Communications* 179, 449–456, 2008.
- Demiray, H., Weakly nonlinear waves in water of variable depth: Variable-coefficient Korteweg-de Vries equation. *Comput. Math. Appl.* 60, 1747–1755, 2010.
- Demiray, H., A note on the wave propagation in water of variable depth. *Applied Mathematics and Computation* 218, 2294–2299, 2011.
- Drazin, P.G., Johnson, R.S., *Solitons: An Introduction*, 2nd ed. Cambridge University Press, 1989.
- Ivancevic, V.G., Ivancevic, T.T., *High-dimensional chaotic and attractor systems a comprehensive introduction*. Springer, Dordrecht, 2007.
- Kassam, A.-K., Trefethen, L.N., Fourth-Order Time-Stepping for Stiff PDEs. *SIAM Journal on Scientific Computing* 26, 1214, 2005.
- Klein, C., Fourth order time-stepping for low dispersion Korteweg-de Vries and nonlinear Schrödinger equations. *Electronic Transactions on Numerical Analysis: Etna*, v.29, 116-135, 2008.
- Korteweg, D. J.; de Vries, G., On the change of form of long waves advancing in a rectangular canal, and on a new type of long stationary waves, *Philosophical Magazine*, 39: 422–443, 1895.
- Krogstad, S., Generalized integrating factor methods for stiff PDEs. *J. Comput. Phys.*, 203(1), pp.72–88, 2005.
- Martinez, P., Legnani, W., Bucci, C., Numerical calculation of conservation laws in solitonic interaction. *Mecánica Computacional Vol XXIX*, págs. 2427-2438, 2010.
- Russell, J.S., Report on Waves. 14th meeting of the British Association for the Advancement of Science, BAAS, London, 1844.
- Tang, S., Zheng, J., Wang, Z., The integral factor method for solving a class of generalized KdV equation. *Applied Mathematics and Computation*, 211(1), pp.185-189, 2009.
- Trefethen, L.N., *Spectral methods in MATLAB*, SIAM, 2000.
- Whitham, G.B., *Linear and Nonlinear Waves*, Wiley, 1974.
- Zabusky, N.J., Kruskal, M.D., Interaction of “Solitons” in a Collisionless Plasma and the Recurrence of Initial States. *Physical Review Letters*, 15(6), pp.240–243, 1965.